

Preparation of Anion Exchange Membrane Based on Homogeneous Quaternization of Bromomethylated Poly(arylene ether sulfone)

Chengji Zhao,¹ Wenjia Ma,² Wenmo Sun,¹ Hui Na¹

¹Alan G. MacDiarmid Institute, College of Chemistry, Jilin University, Changchun 130012, People's Republic of China

²Dalian Institute of Chemical Physics, Chinese Academy of Sciences, Dalian 116023, China

Correspondence to: C. Zhao (E-mail: zhaochengji@jlu.edu.cn)

ABSTRACT: This article presented the synthetic and preparation route of quaternary ammonium functionalized anion exchange membranes (AEMs), which were derived from an engineering plastics polymer, poly(arylene ether sulfone) with 3,3',5,5'-tetramethyl-4,4'-dihydroxybiphenyl moiety (PAES-TM). The benzylmethyl groups on the main-chain of PAES-TM were converted to the bromomethyl groups *via* a radical reaction, thereby avoiding complicated chloromethylation, which required carcinogenic reagents. The chemical structure of the bromomethylated PAES was characterized by ¹H NMR spectrum. Following a homogeneous quaternization with trimethylamine in the solution, a series of flexible and tough membranes were obtained by a solution casting and anion exchange process. The ion exchange capacity values were ranging from 1.03 to 1.37 meq g⁻¹. The properties of the membranes, including water uptake, hydroxide conductivity, and methanol permeability were evaluated in detail. The AEM showed a high conductivity above 10⁻² S cm⁻¹ at room temperature and extremely low methanol permeability of 4.16–4.94 × 10⁻⁸ cm² s⁻¹. The high hydroxide conductivity of TMPAES-140-NOH could be attributed to the nano-scale phase-separated morphology in the membrane, which was confirmed by their transmission electron microscopy images. © 2013 Wiley Periodicals, Inc. *J. Appl. Polym. Sci.* **2014**, *131*, 40256.

KEYWORDS: batteries and fuel cells; copolymers; membranes; swelling

Received 8 June 2013; accepted 3 December 2013

DOI: 10.1002/app.40256

INTRODUCTION

Polymer electrolyte membrane fuel cells (PEMFCs) have been considered to be promising energy conversion devices to resolve the recent energy crisis and environment problems, due to their high energy densities, high conversion efficiencies along with low pollution levels.^{1–3} Polymer electrolyte membrane (PEM) is one of the most important components in PEMFCs, which requires high proton conductivity, excellent chemical stability as well as low cost. Perfluorosulfonic acid copolymers, such as Nafion, are traditionally the membranes of choice in PEMFCs. However, most of acid PEMs including Nafion suffered from two critical deficiencies: (1) the low electrocatalytic efficiency of methanol at the anode, (2) the high crossover of fuel through the membrane.^{4,5} Many investigators have developed various alternative membranes for applications in anion exchange membrane fuel cells (AEMFCs). Unlike current acid PEMs, benefiting from the alkaline media, the electrocatalysis properties of anion exchange membranes (AEMs) could be greatly improved, thereby allowing using non-noble and low-cost metal electrocatalysts in AEMFCs. Moreover, AEMFCs can offer fuel flexibility (*e.g.*, methanol, ethanol, ethylene glycol, etc.), and reduce the undesirable fuel crossover.⁶

Commercial available AEMs are typically based on cross-linked chloromethylated polystyrene or poly(vinylbenzyl chloride).^{7–9} However, the ionic conductivities of these commercial membranes are too low to be used in a high performance solid-state fuel cell. Several groups have reported the preparation of AEMs based on quaternary ammonium functionalized polysulfone, which required a chloromethylation procedure following by aminating with trimethylamine (TMA).^{10–14} The drawbacks of chloromethylation procedure are the large excess of toxic chloromethyl methyl ether reagent and the poor controllability of the chloromethylation position and quantity.¹⁰ Therefore, it has prompted a wide variety of studies on the novel approaches to achieve new polymer architectures for AEMFCs. Methyl-containing polysulfones and polyphenylene polymers have been bromomethylated using *N*-bromosuccinimide (NBS) as the halomethylation agent, which is a much safer and more controllable process.^{15,16} Then, the cast membranes were quaternized by immersing into TMA solution. However, the conversion of bromomethyl groups to benzyltrimethylammonium groups was incomplete. The quaternization process preferred to take place on the surface of membrane rather than in the bulk. So, the quaternization of already-cast and dried membrane in the solid state reduced the quantitative repeatability

of the target-specific degrees of functionality. Therefore, it is important to develop a more quantitative, rapid, and selective method for the preparation of AEMs.

In this study, an aromatic poly(arylene ether sulfone) with benzylmethyl moieties (PAES-TM) was first synthesized by the aromatic nucleophilic polycondensation of 3, 3', 5, 5'-tetramethyl-4, 4'-biphenol (TMBP) and 4,4'-dichlorodiphenyl sulfone. It has been reported that PAES-TM displays high thermal stability, advanced mechanical properties, and excellent resistance to hydrolysis and oxidation.^{17,18} Secondly, the bromomethylated PAES-TM (BrTMPAES) was prepared using NBS as the halomethylation agent. Thirdly, a homogeneous quaternization of bromomethylated PAES by adjusting the addition of TMA provided the flexible and tough alkaline AEMs with various ammoniation degrees. Compared to the quaternization of already-cast membrane in solid state, the homogeneous ammoniation method is more quantitative, rapid, and selective to prepare AEMs. The properties, such as morphology, water uptake (WU), swelling ratio, hydroxide conductivity, methanol permeability, and alkaline stability were then investigated in detail.

EXPERIMENTAL

Materials

TMBP was purchased from Lanzhou Aokai chemical company and used without any further purification. 4,4'-Dichlorodiphenyl sulfone was purchased from Yanbian Longjing chemical company. Benzoyl peroxide as an initiator and NBS as a halomethylation agent were obtained from Shanghai Jiachen chemical company and dried at 80°C for 24 h before use. TMA was obtained from Sinopharm Chemical Reagent. All other solvents were obtained from Tianjin Tiantai chemical company and treated by a standard method prior to use.

Synthesis and Bromomethylation of Poly(arylene ether sulfone) Containing Benzylmethyl Moieties

PAES-TM was synthesized according to a procedure reported by our previous work.¹⁹ A typical procedure was described as follows: a 500 mL three-necked flask was equipped with a mechanical stirrer, a Dean-Stark trap with a reflux condenser, and purged with pure nitrogen. Then TMBP (12.12 g, 50 mmol), 4,4'-dichlorodiphenyl sulfone (14.36 g, 50 mmol), anhydrous potassium carbonate (7.59 g, 55 mmol), 66 mL sulfolane, and 30 mL toluene were added to the flask to form a solvent system with a solid concentration of 25 wt %. The reaction mixture was heated and stirred slowly until the toluene beginning to reflux at about 140°C. After keeping this temperature for 3 h, the temperature was raised to 210°C to remove most of water and toluene. After about 6 h, the mixture was precipitated by pouring into water. Then the precipitation was washed with deionized water for several times and dried in a vacuum oven for 24 h.

PAES-TM of 4.2 g (10 mmol) was dissolved in dried chloroform in a 500 mL three-necked flask equipped with a mechanical stirrer, a nitrogen inlet, and a condenser. Then NBS of 16.02 g (9 mmol) and benzoyl peroxide of 0.02 g (0.09 mmol) were added into the three-necked flask. After refluxing at 62°C for 6 h, the mixture was poured into 50% volume fraction of ethanol and water mixture. A pale yellow precipitate was obtained

under vigorous stirring. The precipitate was filtered off, washed with ethanol for three times, and then purified in vacuum.

Preparation of AEMs Based on Quaternary Ammoniation of BrTMPAES

A typical preparation procedure of TMPAES-*x*-NOH AEMs was described as follows: a 250 mL three-neck round-bottomed flask equipped with a nitrogen inlet and a dropping funnel was charged with BrTMPAES (4.94 g, 5 mmol) and *N,N*-dimethylacetamide to form a 8% (w/v) solution. Then quantitative TMA (80, 100, 120, or 140% equiv. molar of benzylmethyl moieties on the polymer) was slowly dripped into the solution from the dropping funnel. By adjusting the addition of TMA, a homogeneous solution of TMPAES-*x*-NBr was obtained after constantly stirring of the mixture at 40°C for 4 days. Then the resulted solution was equipped with a pressure-relief device to remove the vestige of TMA at room temperature and subsequently casted directly onto a clean glass plate. After carefully dried at room temperature for 3 h and vacuum-dried at 120°C for 24 h, tough and flexible membranes of TMPAES-*x*-NBr with different ion exchange capacities (IECs) were obtained. The membranes were transformed to the hydroxide form (TMPAES-*x*-NOH) by anion exchange in 1M NaOH aqueous solution for 24 h at room temperature. Then, the membranes were soaked and washed thoroughly with deionized water under the protection of N₂. The thickness of membranes were in the range 60–80 μm.

Characterization

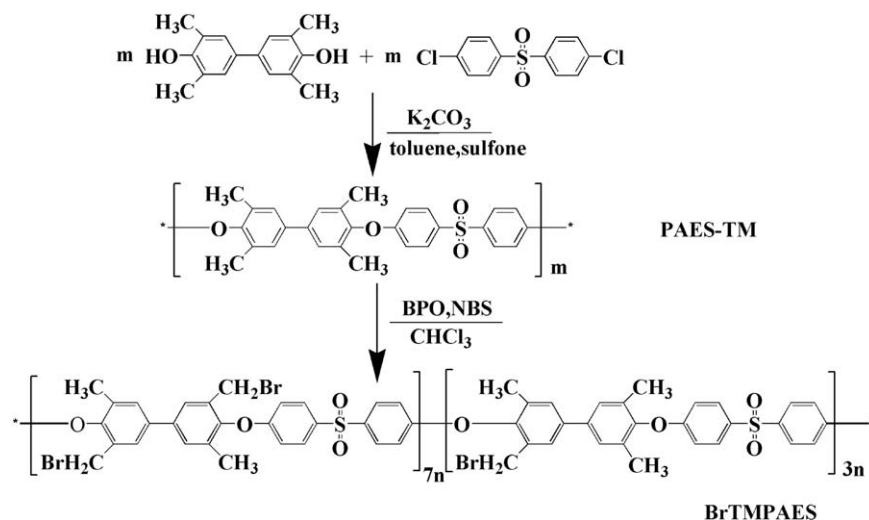
Measurements. ¹H NMR spectrum was recorded on a Bruker 400 MHz spectrometer using deuterated chloroform (CDCl₃-*d*₆) to confirm the chemical structure of BrTMPAES. The bromine content per repeat unit of the BrTMPAES, *D*_{Br}, is evaluated by integration and comparison of the ¹H NMR signals arising from the methyl protons and the brominated methylene protons. *D*_{Br} was calculated by the following eq. (1):

$$D_{\text{Br}} = \frac{12A_{\text{Hd}}}{3A_{\text{Hd}} + 2A_{\text{He}}} \quad (1)$$

where *A*_{Hd} is the peak area of the brominated methyl protons and *A*_{He} corresponds to the peak area of the methylene protons. Thermogravimetric analysis (TGA) was performed in nitrogen with a Pyris 1-TGA (Perkin-Elmer) thermogravimetric analyzer at a heating rate of 10°C min⁻¹ from 80 to 750°C. To investigate the mechanical properties of membranes, the tensile measurement was carried out at room temperature at a constant crosshead speed of 2 mm min⁻¹. The uniaxial tensile measurement was conducted on the membrane samples with 4 mm width and 15 mm length.

Transmission Electron Microscopy. The cross-sectional TEM images were determined by JEM-2000EX (JEOL) using an accelerating voltage of 200 kV. Before test, the membrane was first dyed with PdCl₄²⁻ by immersing into a 0.02 M PdCl₄²⁻/HCl solution for 24 h, and then rinsed with excessive water and finally dried at room temperature for 12 h.

IEC, WU, and Membrane Swelling. The membranes in OH⁻¹ form were immersed in accurate 20 mL of HCl solution for 48 h. The solution was then titrated with a standard NaOH solution using phenolphthalein as an indicator. Then IEC was calculated by the following equation:



Scheme 1. Synthetic route of poly(arylene ether sulfone) based on TMBP.

$$\text{IEC (meq g}^{-1}\text{)} = \frac{C_{\text{HCl}} \times V_{\text{HCl}} - C_{\text{NaOH}} \times V_{\text{NaOH}}}{M} \quad (2)$$

where C_{HCl} is the molar concentration of HCl solution, V_{HCl} is the volume of HCl solution, C_{NaOH} is the molar concentration of NaOH solution, V_{NaOH} is the volume of NaOH solution, and M corresponds to the weight of dried membrane.

The WU and membrane swelling (MS) ratio were determined by measuring the change in the weight and dimensional change between the dry and wet membranes, respectively. A detailed procedure was reported previously.¹⁹ The WU and MS of the membranes was calculated according to eq. (3):

$$\text{WU} = \frac{W_{\text{wet}} - W_{\text{dry}}}{W_{\text{dry}}} \times 100\%$$

$$\text{MS} = \frac{L_{\text{wet}} - L_{\text{dry}}}{L_{\text{dry}}} \times 100\% \quad (3)$$

W_{dry} and W_{wet} are the weight of the dry and the corresponding water-swollen membranes, respectively. L_{dry} and L_{wet} are the length of the dry and the corresponding water-swollen membranes, respectively.

Hydroxide Conductivity. The in-plane hydroxide conductivity of TPAES- x -NOH membranes was determined by a modified four-probe AC impedance method from 0.1 Hz to 100 kHz, 10 mV AC perturbation, and 0.0 V DC rest voltage using a Princeton Applied Research Model 2273 potentiostat/galvanostat/FRA. The membranes and the electrodes were set in a Teflon cell and the distance between the reference electrodes was 1 cm. The cell was placed in a thermo-controlled chamber in liquid water for measurement. The impedance measurement was performed from 20 to 70°C under 100% relative humidity. The hydroxide conductivity (σ , S cm⁻¹) of membranes was calculated according to eq. (4):

$$\sigma = \frac{L}{R \cdot A} \quad (4)$$

where L is the distance between reference electrodes, R is the membrane resistance, and A is the cross-sectional area of membrane.

Alkaline Stability. The alkaline stability of the membranes was evaluated in 0.01, 0.1, 1 and, 6M NaOH solution at 60°C, respectively. The percentage of degradation (x) was expressed as:

$$x = \frac{M_a - M_b}{M_a} \times 100\% \quad (5)$$

where M_a was the weight predegradation test in different concentrations of NaOH solution and M_b was the weight after the degradation test.

Methanol Permeability. Methanol permeability was determined using a home-made diffusion cell, which was composed of two reservoirs, each with a capacity of approximately 200 mL, separated by a vertical membrane.¹⁹ Prior to the test, the membranes were immersed in deionized water for at least 12 h. Initially, reservoir V_A contained 10M methanol and water solution, and reservoir V_B contained pure deionized water. The magnetic stirrers were used continuously during the measurement. Methanol concentrations in the water cell were determined using a SHIMADZU GC-8A chromatograph. Methanol permeability was calculated by eq. (6):

$$C_B(t) = \frac{A \text{ DK}}{V_B L} C_A(t - t_0) \quad (6)$$

where A (cm²), L (cm), and V_B (mL) are the effective area, the thickness of the membranes, and the volume of permeated reservoirs, respectively. C_A and C_B (mol m⁻³) are the methanol concentration in feed and in permeate, respectively. DK (cm² s⁻¹) denotes the methanol permeability.

RESULTS AND DISCUSSION

Synthesis of Bromomethylated Poly(arylene ether sulfone)

The synthetic procedure of PAES-TM and bromomethylated poly(arylene ether sulfone) is shown in Scheme 1. The conversion of the benzylmethyl groups to the bromomethyl groups was adjusted by controlling the amount of NBS. The reaction proceeded efficiently in the refluxing CHCl₃, then a pale yellow powder of the brominated polymer was obtained after precipitation. The reaction temperature was kept at 62°C, the reaction time was set to 6 h, and 0.05 equiv. of benzoyl peroxide initiator was used. The degree of

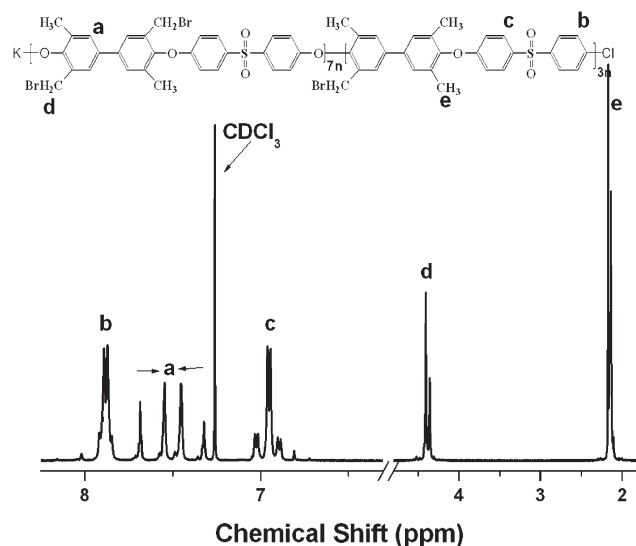


Figure 1. ^1H NMR spectrum of bromomethylated poly(arylene ether sulfone) in CDCl_3 .

functionality was calculated by ^1H NMR spectroscopic technique. As shown in Figure 1, the peaks at about δ 2.17 ppm were assigned to the methyl groups and the peaks at about δ 4.40 ppm were attributed to the proton of bromomethylenes. The integration ratio of H_d-H_e was used to calculate the degree of bromination. For the synthesized BrTMPAES, the integration ratio of the H_d-H_e was 0.48, and the D_{Br} was calculated to be 1.7, indicating a BrTMPAES with approximate 1.7 bromine atoms per repeating unit was obtained.

Preparation of AEMs Based on Quaternary Ammoniation of BrTMPAES

As shown in Scheme 2, the content of quaternary ammoniation of BrTMPAES was controlled simply by the feed ratio of TMA to the benzylmethyl moieties on the polymer. The ammoniation degree of TMPAES- x -NBr membranes increased with the TMA concentration increasing. Then, the TMPAES- x -NBr membranes

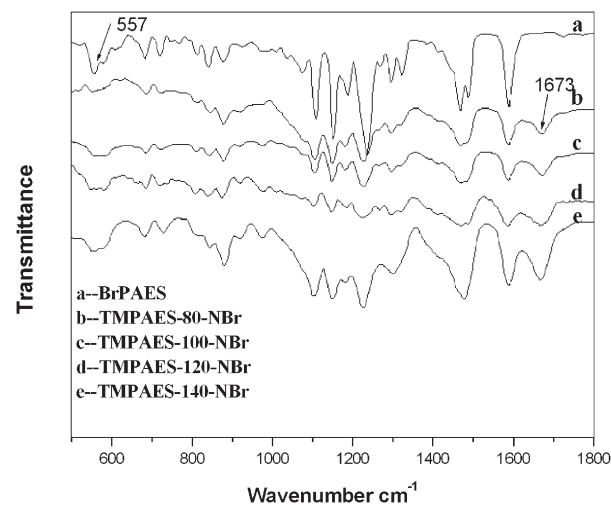
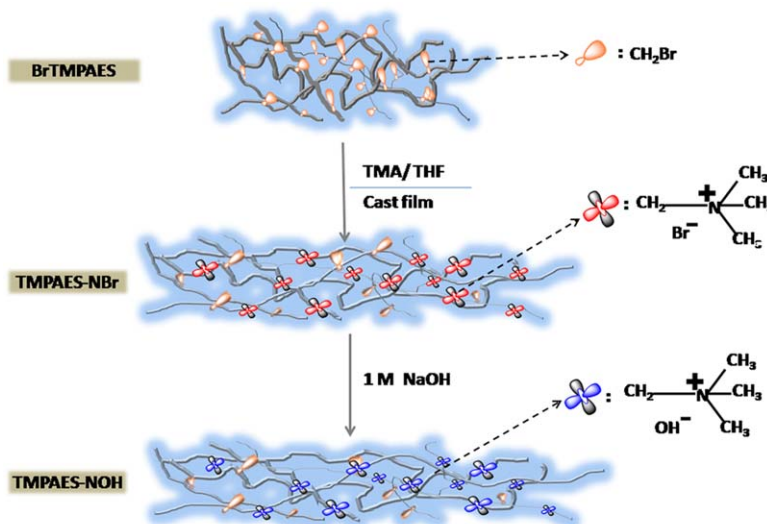


Figure 2. FTIR spectra of bromomethylated poly(arylene ether sulfone) and ammoniated poly(arylene ether sulfone).

were transformed to OH^- forms by immersing in 1M NaOH solution. The FTIR spectra of BrTMPAES and TMPAES- x -NBr membranes were recorded and are shown in Figure 2. After the quaternary ammoniation of BrTMPAES, the new characteristic peaks at about 1673 cm^{-1} were clearly observed in Figure 2(b–e). They could be attributed to the C–N stretching of ammonium groups. Meanwhile, the stretching of C–Br bond at 571 cm^{-1} was less obvious than that of BrTMPAES after quaternization reaction. These results confirmed that the quaternization reaction was successful by blending BrTMPAES and TMA in solution, which was called as a homogeneous ammoniation method.

Table I lists the solubility of BrTMPAES and TMPAES- x -NBr in common solvent. BrTMPAES were insoluble in xylene, DMSO, ethyl ether, alcohol, and butanone, but could be soluble in NMP, chloroform, and THF at room temperature. TMPAES- x -NBr were soluble in NMP and DMSO at the temperature above



Scheme 2. Bromomethylation and ammoniation of poly(arylene ether sulfone). [Color figure can be viewed in the online issue, which is available at wileyonlinelibrary.com.]

Table I. Solubility Properties of BrTMPAES and TMPAES-*x*-NBr Membranes

Solvents	Chloroform	Xylene	THF	DMSO	NMP	Ethyl ether	Alcohol	Butanone
BrTMPAES	+	–	+	–	+	–	–	–
TMPAES-80-NBr	–	–	–	+-	+-	–	–	–
TMPAES-100-NBr	–	–	–	+-	+-	–	–	–
TMPAES-140-NBr	–	–	–	+-	+-	–	–	–
TMPAES-160-NBr	–	–	–	+-	+-	–	–	–

Solubility: (+) soluble, (–) insoluble, (+–) soluble by heating.

80°C, but could not be insoluble in any other solvents. One drawback for AEMFCs is the lack of a soluble ionomer that can be used in the catalyst layer to build an efficient three-phase boundary. The solubility of TMPAES-*x*-NBr in DMSO and NMP provides them to be used as ionomers, which could improve the utilization of the catalyst particles and reduce the internal resistance.

Morphology

TEM was carried out on the TMPAEK-*x*-NOH membranes after staining with PdCl₄^{2–} anion to investigate their morphology and phase separation (Figure 3).^{20–22} In these TEM images, the dyed hydrophilic domains appeared as dark regions due to their affinity with PdCl₄^{2–} anions, and the white regions were assigned to the hydrophobic domains in the membranes. As can be seen in Figure

3, the ionic clusters of TMPAEK-*x*-NOH membranes recognized as dark spots were homogeneously penetrated into the hydrophobic background. The morphology is very similar to quaternized poly(aryl ether sulfone)s reported by Zhuang's group²¹ and Zhang's group.²² The density as well as the average size of ionic clusters in the TMPAEK-*x*-NOH membranes exhibited a gradual increase with the quaternary ammonium content increasing, indicating that a higher ionic content resulted in a larger hydrophilic domain and thus a large ionic conducting channel. The kind of hydrophilic/hydrophobic microphase separation morphology was considered to be essential for good ionic conductivity.

IEC, WU, and MS

The IECs of TMPAES-*x*-NOH membranes were tested and the values are listed in Table II. As expected, they increased with

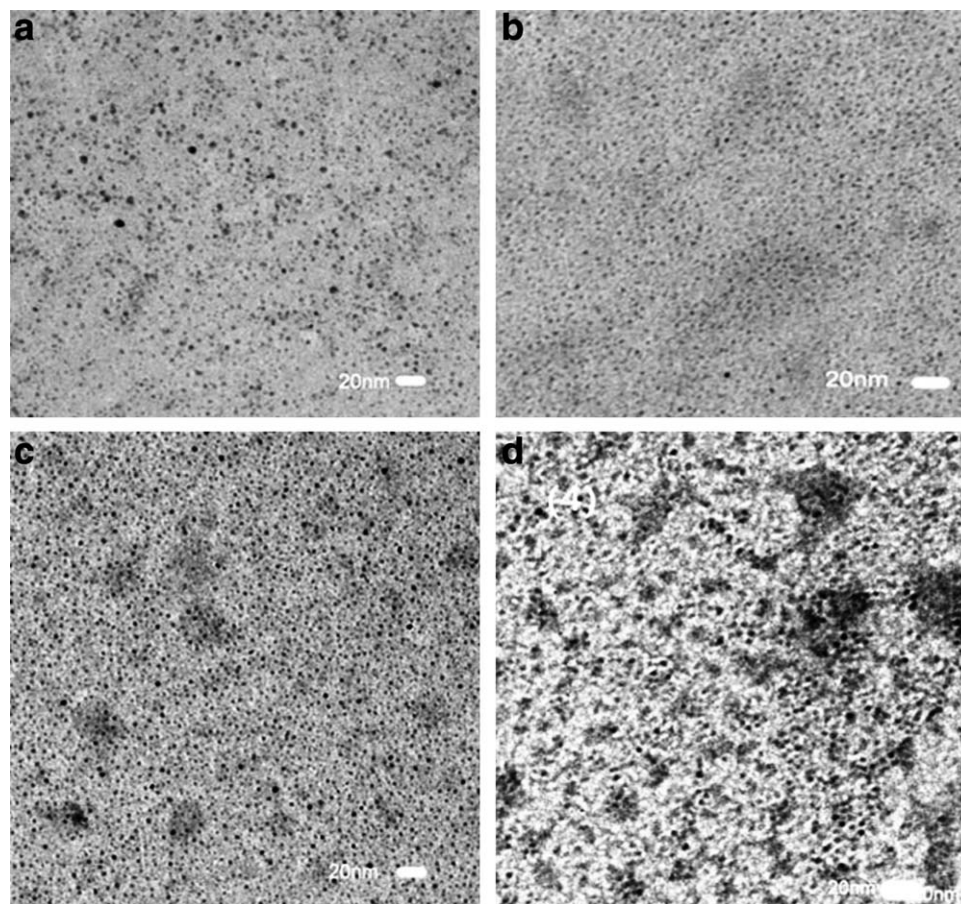


Figure 3. TEM micrographs of polymer membranes: (a) TMPAES-80-NOH; (b) TMPAES-100-NOH; (c) TMPAES-120-NOH; and (d) TMPAES-140-NOH.

Table II. IEC, Water Uptake, Membrane Swelling, Methanol Permeability, and Hydroxide Conductivity (σ) of the TMPAES-*x*-NOH Membranes

Membrane	Thickness (μm)	WU		MS		IEC (meq g^{-1})	DK ($\times 10^{-8} \text{cm}^2 \text{s}^{-1}$)	σ (S cm^{-1}) 70°C
		20°C	70°C	20°C	70°C			
TMPAES-80-NOH	60	21.2	27.9	6.4	9.7	1.03	4.94	0.016
TMPAES-100-NOH	80	24.6	37.0	8.7	12.6	1.09	4.11	0.032
TMPAES-120-NOH	65	26.4	38.3	9.3	17.1	1.12	4.72	0.039
TMPAES-140-NOH	75	28.2	42.0	10.5	20.4	1.37	4.16	0.054

increasing the ammoniation degree. According to the investigations of Yanagi and Fukuta,²³ AEMs in OH^{-1} forms would be gradually converted into bicarbonate form on exposure to air as a result of the rapid absorption of CO_2 . Meanwhile, the conductivity of the membranes could steadily decline over a period of few days due to the sorption of CO_2 . To avoid the influence of HCO_3^- , the AEMs were sealed and protected by N_2 during the ionic conversion before all the characterization.

As is well known, WU has a profound effect on the conductivity and mechanical properties of PEMs. Water molecules dissociate the alkaline functionality and facilitate hydroxide transport. However, excessively high levels of WU can result in membrane fragility and dimensional change. Table II shows the WU and MS ratios of TMPAES-*x*-NOH membranes at different temperatures. As expected, the water sorption of these membranes increased with IEC increasing due to the strong hydrophilicity of the ammonium groups. An increase in WU with temperature increasing was also observed. Most of the membranes exhibited the moderate WU in the range 21.2–52.6%, indicating that these membranes have a reliable dimensional stability.

Thermal Stability

To investigate the effect of ammonium group on the thermal stability of TMPAES-*x*-NOH, typical curves of BrTMPAES and TMPAES-*x*-NOH membranes are shown in Figure 4. The

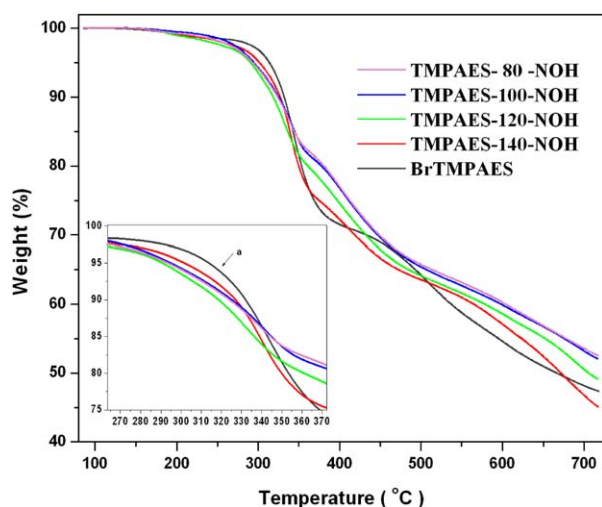


Figure 4. TGA curves for bromomethylated poly(arylene ether sulfone) and poly(arylene ether sulfone) with ammonium group. [Color figure can be viewed in the online issue, which is available at wileyonlinelibrary.com.]

BrTMPAES membranes exhibit a two-step degradation. The first decomposition temperature corresponding to the C–Br bond cleavage is at about 278°C, while the second decomposition temperature at about 436°C is believed to be associated with the main-chain degradation. The TMPAES-*x*-NOH membranes exhibit a lower decomposition temperature than that of the C–Br bond cleavage at 240°C, which is related to the internal water because of strong hydrophilicity of the benzyltrimethyl ammonium group. At about 310°C [Figure 4(a)], TMPAES-*x*-NOH have a slight change in degradation rates, which is considered to be the temperature of benzyltrimethyl ammonium group decomposition. Especially, TMPAES-140-NOH with the most benzyltrimethyl ammonium groups has the fastest degradation rate. It is believed that the main-chain decomposition happened at about 430°C. The AEMs exhibit a thermo-tolerant temperature higher than 200°C, which was high enough for the potential applications in AEMFCs.

Mechanical Properties

The mechanical properties of TMPAES-*x*-NBr and TMPAES-*x*-NOH membranes are summarized in Table III. The samples in the bromine form (TMPAES-*x*-NBr) have tensile stress at maximum load of 15.6–29.3 MPa, Young's modulus of 560.2–1049.6 MPa, and elongation at break of 5.56–12.75%. For the TMPAES-*x*-NBr membranes, the tensile stress, and the Young's modulus of samples both decrease with the content of benzyltrimethyl ammonium groups increasing. It is because that the introduction of strong polar benzyltrimethyl ammonium

Table III. Mechanical Properties of TMPAES-*x*-NBr and TMPAES-*x*-NOH Membranes

Membrane	Tensile modulus (MPa) ^a	Elongation break (%)	Tensile strength (MPa)
TMPAES-80-NBr	1049.6	7.16	29.3
TMPAES-100-NBr	1024.1	5.56	25.5
TMPAES-120-NBr	812.1	7.26	19.4
TMPAES-140-NBr	560.2	12.75	15.6
TMPAES-80-NOH	866.3	5.13	22.8
TMPAES-100-NOH	487.3	5.67	15.1
TMPAES-120-NOH	321.7	2.62	6.9
TMPAES-140-NOH	164.9	1.09	2.1

^a Membranes were immersed in water for 24 h and tested immediately.

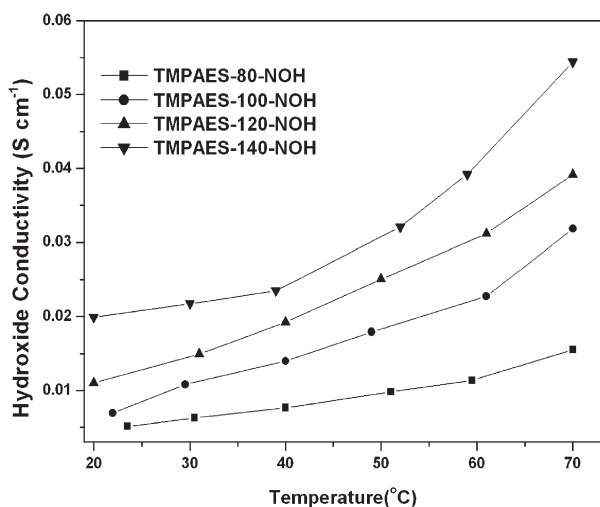


Figure 5. Hydroxide anion conductivity of TPAES-*x*-NOH membranes at different temperatures under fully hydrated conditions.

groups in side chains damage the ordering of aggregative state of TPAES backbone, and thus reduce the mechanical strength of the aromatic polymers. Furthermore, TPAES-*x*-NBr membranes show a decrease then increase in elongation at break as the content of benzyltrimethyl ammonium groups increase. On the one hand, the mechanical properties of the aromatic polymers was reduced by introducing ammonium groups. On the other hand, the TPAES-*x*-NBr membranes could absorb more water molecules under ambient condition, which functioned as plasticizers to improve the flexibility of the membranes.

For the TPAES-*x*-NOH membranes, all of the tensile stresses, elongations at break, and Young's modulus of the samples decreased with the content of quaternary ammonium groups increasing. Moreover, the mechanical stability of TPAES-*x*-NOH membranes decreased significantly compared with TPAES-*x*-NBr. It can be attributed to both the sorption of water and degradation of the polysulfone backbone in alkaline condition. The hydrogen-bond interaction between the water molecules and the quaternary ammonium hydroxide groups is much higher than that between water molecules and bromine atoms, which result in a further increase of WU and swelling properties of TPAES-*x*-NOH membranes, which in turn

would reduce intermolecular forces and consequently deteriorate the mechanical strength of the membranes.

Hydroxide Conductivity

The hydroxide conductivities of TPAES-*x*-NOH membranes were measured at 100% RH and the conductivities are presented in Figure 5. The membranes were immersed in liquid water and the impedance measurements were performed for every 10° from room temperature to 70°C. As expected, the conductivity increased as the benzyltrimethyl ammonium groups increased. As the IEC increasing, the hydroxide conductivity of TPAES-*x*-NOH membranes increases from 5.4 to 20 mS cm⁻¹ at room temperature. It is also observed from Figure 5 that the hydroxide conductivity increased with temperature. For example, TPAES-140-NOH with the highest IEC had a highest conductivity of 54 mS cm⁻¹ at 70°C. TPAES-*x*-NOH membranes were then compared with the literature reported AEMs, which were based on various polymeric materials bearing quaternary ammonium groups. Table IV lists the IEC, hydroxide conductivities, and methanol permeability of these membrane materials, which are the most properties for application in DMFCs.^{24–31} It is seen that our fabricated TPAES-140-NOH membrane exhibit the hydroxide conductivity that are close to or higher than most of AEMs reported. To the best of our knowledge, most of the reported AEMs were converted by immersing the completely dried membrane in TMA in water in a sealed container for 48 h at room temperature to convert the bromomethylbenzyl groups to quaternary ammonium moieties in the membrane. The distribution of ammonium groups in AEMs from heterogeneous amination could not be as homogeneous as the membranes formed by solution reaction method. Homogeneous amination made the ionic groups randomly distribute along the polymer backbone chains, which was confirmed by their TEM images stained by palladium. As pointed by previous work,³² water resided in benzyltrimethyl ammonium groups along polymer chains will deliver hydroxide, therefore, the homogeneously distribution of cationic groups would enhance the hydroxide conductivity of TPAES-*x*-NOH membranes.

Methanol Permeability

Table II also lists the methanol permeability of TPAES-*x*-NOH membranes. The methanol permeability increases with IEC and WU values increasing. TPAES-*x*-NOH membranes

Table IV. IEC, Hydroxide Conductivity, and Methanol Permeability of AEMs Reported in the Literature

Membrane materials	IEC (meq g ⁻¹)	σ (mS cm ⁻¹)	DK (cm ² s ⁻¹)	Ref.
TPAES-140-NOH	1.37	20 (20°C)	4.94×10^{-8} (20°C)	This work
APSEBS	0.578	0.69 (20°C)	Not reported	24
QSEBS	0.3	5 (30°C)	4.45×10^{-7} (30°C)	25
Pore-filling AM-APS	3.0	4.8 (60°C)	7.5×10^{-8} (25°C)	26
QAPVA	Not reported	2.76–7.34 (30°C)	$1.0\text{--}4.1 \times 10^{-6}$ (30°C)	27
PVA-AESP	1.21–1.76	35–76 (30°C)	$2.03\text{--}4.12 \times 10^{-7}$ (30°C)	28
CPPO-40	1.0	15.3 (25°C)	1.12×10^{-7} (25°C)	29
SPES-2OH	Not reported	18.8 (20°C)	1.92×10^{-9} (20°C)	30
QPPEK-OH	Not reported	1.2 (22°C)	7.21×10^{-7} (22°C)	31

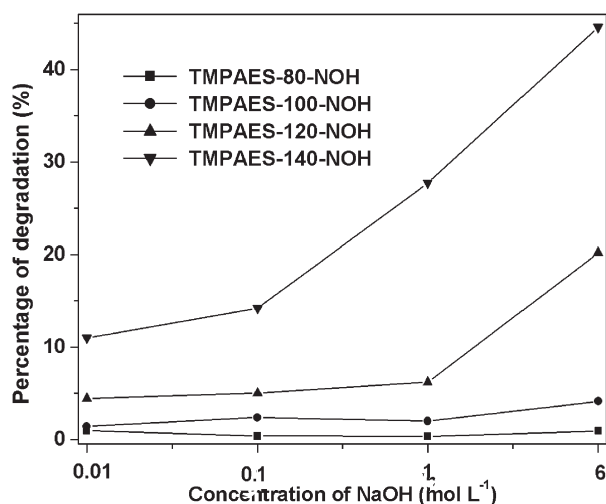


Figure 6. Degradation properties of poly(arylene ether sulfone) with ammonium group in NaOH solutions.

show the methanol permeability of $4.16\text{--}4.94 \times 10^{-8} \text{ cm}^2 \text{ s}^{-1}$, much lower than those of Nafion 117 ($1.0 \times 10^{-6} \text{ cm}^2 \text{ s}^{-1}$) and other proton exchange membranes. In the alkaline methanol fuel cell, the ionic current flows from the cathode to the anode, which is reverse to the direction of methanol crossover and reduces the methanol cross-over. As listed in Table IV, the methanol permeability of AEMs in the literature is mainly around $10^{-7}\text{--}10^{-9} \text{ cm}^2 \text{ s}^{-1}$. The results of TMPAES-*x*-NOH membranes proved again that the AEMs could inhibit the flow of methanol successfully.

The selectivity (the ratio of proton conductivity to methanol permeability) was also calculated to evaluate the potential performance of direct methanol fuel cell membranes. The selectivity of TMPAES-*x*-NOH membranes increased from 0.8×10^5 to $4.8 \times 10^5 \text{ S s cm}^{-3}$ with the IEC increasing from 1.03 to 1.37 meq g⁻¹. The higher selectivity ratio indicated that the TMPAES-*x*-NOH membranes could be promising AEMs for direct methanol fuel cells.

Alkaline Stability

The key property for AEMs in fuel cells is the chemical stability of the cationic groups. Even in an electrochemical cell without any added electrolyte, the localized pH within the membrane is quite high enough to lead to chemical attack on the quaternary ammonium groups. A stability study of quaternization ammoniation group was reported by Varcoe et al.³³ A 233 h durability test of AEM with benyltrimethylammonium cationic groups was taken, only a 5% decrease trend of an ion-exchange capacity under operating conditions was observed, indicating a reasonable stability under the operating conditions.

The alkaline stability of TMPAES-*x*-NOH membranes was conducted by immersing samples in a series of aqueous solutions of NaOH with different concentrations held at 60°C for 24 h. As seen from Figure 6, an increase in the weight loss was observed with the increasing concentration of NaOH solution. A decrease in alkaline stability was also observed with increasing quaternary ammonium group contents in AEMs. At lower IEC, TMPAES-80-NOH and TMPAES-100-NOH could maintain rea-

sonable alkaline stability at a wide range of pH values. Even after 120 h exposure to 1 or 6M NaOH at 60°C, the percentage of degradation was still lower than 5%. However, the weight of TMPAES-120-NOH decreased by 28% after treatment with 6M NaOH at 60°C, and the weight of TMPAES-140-NOH decreased by 45%. These observations implied that quaternary ammonium cations were degraded at higher IEC. As reported,³⁴ the degradation of them in alkaline solution at high temperature is mainly due to the nucleophilic substitution reaction, in which the hydroxides attack the α -carbon of the ammonium cations.

CONCLUSIONS

A series of novel AEMs TMPAES-*x*-NOH were prepared from bromomethylation and homogeneous amination process of TMBP-based poly(arylene ether sulfone). The bromomethylation of poly(arylene ether sulfone) by NBS was proved to be a rapid and convenient method. The homogeneous amination process provides an efficient and controllable method to prepare AEMs. By controlling the degree of functionalization on the polymers, AEMs with a wide range of WU values and ionic conductivities can be prepared. These AEMs based on poly(arylene ether sulfone)-bearing benzylmethyl groups exhibited methanol permeability $<10^{-7} \text{ cm}^2 \text{ s}^{-1}$ as well as high selectivity. Moreover, the hydroxide conductivity of TMPAES-140-NOH is 54 mS cm^{-1} at 70°C, that is comparable to those of traditional AEMs based on heterogeneous amination. These membranes showed a reasonable alkaline stability at lower quaternary ammonium contents. At higher content, the quaternary ammonium cations were degraded due to the nucleophilic substitution reaction. We will carry out further work to explore the possibility of incorporating other kinds of tertiary amine-containing compounds such as guanidine, imidazolium-based cations to improve the alkaline stability at higher IEC for applications in AEMFCs.

ACKNOWLEDGMENTS

The authors gratefully acknowledge the financial support of this work by Natural Science Foundation of China (Grant no. 21104022) and Jilin University Basic Research Founding (No: 450060481017).

REFERENCES

- Lu, S.; Pan, J.; Huang, A.; Zhuang, L.; Lu, J. *Proc. Natl. Acad. Sci. USA* **2008**, *105*, 20611.
- Winter, M.; Brodd, R. *J. Chem. Rev.* **2004**, *104*, 4245.
- Hickner, M. A.; Ghasseni, H.; Kim, Y. S.; Einsla, B. R.; McGrath, J. E. *J. Chem. Rev.* **2004**, *104*, 4587.
- Stoica, D.; Ogier, L.; Akrou, L.; Alloin, F.; Fauvarque, J. F. *Electrochim. Acta* **2007**, *53*, 1596.
- Wang, Z.; Chang, H.; Ni, H. Z.; Wu, Q. H.; Zhang, M. Y.; Zhang, H. X. *J. Appl. Polym. Sci.* **2011**, *120*, 914.
- Asazawa, K.; Yamada, K.; Tanaka, H.; Oka, A.; Taniguchi, M.; Kobayashi, T. *Angew. Chem. Int. Ed.* **2007**, *46*, 8024.
- Kostov, G.; Turmanova, S. *J. Appl. Polym. Sci.* **1997**, *64*, 1469.
- Kaur, I.; Barsola, R.; Misra, B. *J. Appl. Polym. Sci.* **1995**, *56*, 1197.

9. Mika, A. M.; Childs, R. F.; Dickson, J. M.; McCarry, B. E.; Gagnon, D. R. *J. Membr. Sci.* **1995**, *108*, 37.
10. Taylor, L. D.; Laughlin, P. M. *J. Appl. Polym. Sci.* **1976**, *20*, 2225.
11. Xiong, Y.; Liu, Q. L.; Zeng, Q. H. *J. Power Sources* **2009**, *193*, 541.
12. Xu, T. W.; Liu, Z. M.; Li, Y.; Yang, W. H. *J. Membr. Sci.* **2008**, *320*, 232.
13. Hou, H. Y.; Sun, G. Q.; He, R. H.; Sun, B. Y.; He, W. J.; Xin L. Q. *Int. J. Hydrogen Energy* **2008**, *33*, 7172.
14. Gu, S.; Cai, R.; Luo, T.; Chen, Z. W.; Sun, M. W.; Liu, Y.; He, G. H.; Yan, Y. S. *Angew. Chem. Int. Ed.* **2009**, *48*, 6499.
15. Hibbs, M. R.; Fujimoto, C. H.; Cornelius, C. J. *Macromolecules* **2009**, *42*, 8316.
16. Yan, J. L.; Hickner, M. A. *Macromolecules* **2010**, *43*, 2349.
17. Gil, M.; Ji, X. L.; Li, X. F.; Na, H.; Hampsey, J. E.; Lu, Y. F. *J. Membr. Sci.* **2004**, *234*, 75.
18. Huang, Z. Z.; Yu, L. M.; Sheng, S. R.; Ge, W. W.; Liu, X. L.; Song, C. S. *J. Appl. Polym. Sci.* **2008**, *108*, 1049.
19. Zhao, C. J.; Lin, H. D.; Na, H. *Int. J. Hydrogen Energy* **2010**, *35*, 2176.
20. Zhang, H. Z.; Zhang, H. M.; Zhang, F. X.; Li, X. F.; Li Y.; Vankelecom, I. *Energy Environ. Sci.* **2013**, *6*, 776.
21. Pan, J.; Lu, S.; Li, Y.; Huang A.; Zhuang, L.; Lu, J. *Adv. Funct. Mater.* **2010**, *20*, 312.
22. Zhang, Q.; Zhang, Q. F.; Wang, J. H.; Zhang, S. B.; Li, S. H. *Polymer* **2010**, *51*, 5407.
23. Yanagi, H.; Fukuta, K. *ECS Trans.* **2008**, *16*, 257.
24. Vinodh, R.; Ilakkiya, A.; Elamathi, S.; Sangeetha, D. *Mater. Sci. Eng. B* **2010**, *167*, 43.
25. Zeng, Q. H.; Liu, Q. L.; Broadwell, I.; Zhu, A. M.; Xiong Y.; Tu, X. P. *J. Membr. Sci.* **2010**, *439*, 237.
26. Jung, H.; Fujii, K.; Tamaki, T.; Ohashi, H.; Ito T.; Yamaguchi, T. *J. Membr. Sci.* **2011**, *373*, 107.
27. Xiong, Y.; Fang, J.; Zeng Q. H.; Liu, Q. L. *J. Membr. Sci.* **2008**, *311*, 319.
28. Tripathi, B. P.; Kumar, M.; Shahi, V. K. *J. Membr. Sci.* **2010**, *360*, 90.
29. Wu, L.; Xu, T. *J. Membr. Sci.* **2008**, *322*, 286.
30. Ni, J.; Zhao, C. J.; Zhang, G.; Zhang, Y.; Wang, J.; Ma, W. J.; Liu, Z. G.; Na, H. *Chem. Commun.* **2011**, *47*, 8943.
31. Zhang, H.; Zhou, Z. *J. Appl. Polym. Sci.* **2008**, *110*, 1756.
32. Chu, P. P.; Wu, C. S.; Liu, P. C.; Wang, T. H.; Pan, J. P. *Polymer* **2010**, *51*, 1386.
33. Varcoe, J. R.; Slade, R. C. T. *Chem. Comm.* **2006**, *5*, 839.
34. Chen, D. Y.; Hickner, M. A. *ACS Appl. Mater. Interfaces*, **2012**, *4*, 5775.